Nanoscale

PAPER

View Article Online
View Journal | View Issue

Cite this: *Nanoscale*, 2015, **7**, 16110

Defect related emission *versus* intersystem crossing: blue emitting ZnO/graphene oxide quantum dots

Sesha Vempati,*[a] Asli Celebioglu[a,b] and Tamer Uyar[a,b]

Received 3rd July 2015,
Accepted 2nd September 2015

DOI: 10.1039/c5nr04461h

www.rsc.org/nanoscale

In ref. [*Nat. Nanotechnol.*, 2012, **7**, 465–471] interesting optoelectronic properties of ZnO/graphene oxide (GO) composite were presented. Essentially, in the luminescence spectrum indirect optical transitions were identified to be from the epoxy group of GO (GO_{epoxy}) to the valance band (E_v) of ZnO. *Viz.* 406 nm, L1: $(LUMO+2)_{GO_{epoxy}} \rightarrow E_v$ and 436 nm, L2: $(LUMO)_{GO_{epoxy}} \rightarrow E_v$. Furthermore, the emission peak at ~550 nm was attributed to zinc interstitials (Zn_is) or oxygen vacancies (V_Os) and shown to span from 350–650 nm (equivalent to a width of ~0.8 eV). In this report we accentuate two vital though largely ignored concerns as itemized in the following. (i) By considering the growth mechanism of ZnO in the composite, there is a certain possibility that these two bands (L1 and L2) may originate from intrinsic defects of ZnO such as Zn_is and extended Zn_is (ex-Zn_is). Or L1 and L2 might be intrinsic to GO. (ii) The 550 nm emission involves V_Os and consists of two components with a typical width of ~0.3 eV. Here we present the results of a thorough investigation confirming the presence of Zn_is, ex-Zn_is and intrinsic emission from GO. We also note that during the synthesis the presence of dimethyl formamide significantly affected the emission from GO in addition to some chemical modifications. Apart from these, we have discussed other crucial factors which require deeper attention in the context of luminescence from complex systems such as those present.

Introduction

In recent years graphene oxide (GO) has attracted a lot of research attention,[1–9] where its potential is evident in its pure form.[2,6,10,11] However, the properties can be enhanced/tuned *via* combinations[2,4,8,9,12–14] especially for optical and optoelectronic applications.[3–5,13] In any case as a prerequisite, a clear understanding of the emission properties is essential for future developments.[2,4,5] For instance, the fluorescence from GO is attributed to the oxygen functional groups (C–O, C═O, and O–C═O) or to the localization of sp^2 carbons.[2,5] While keeping that in mind, in the case of intercalating structures,[2,4] the intricacy of the optical properties is of course not abated, where an overlap of the emission bands is present. Nevertheless, we have recently deconvoluted in the case of a GO/polyaniline intercalating compound despite an overlap of emission lines.[4] It is an undisputed fact that the composites of GO have great potential[2,3,8,9,13,15] when combined with other materials such as ZnO,[2,3] TiO_2,[15] *etc*. The emission properties are strongly dependent on the type of interaction between GO and the other constituent,[2,4,14,15] *e.g.* intersystem crossings in TiO_2/GO by Bao *et al.*[15] and ZnO/GO by Son *et al.*[3] Please refer to ref. 2. for more examples and associated interactions. Among these, the case of ZnO is not only intriguing,[3,16] but also quite intertwined, especially when the fluorescence from GO superpose with the defect related emission of ZnO.[2,16–23] In conjunction with this, we turn our attention to the emission properties of ZnO/GO quantum dots (QDs), precisely to ref. 3. While elucidating the emission properties of GO/ZnO QDs the observed blue emission bands were attributed to transitions L1: $(LUMO+2)_{GO_{epoxy}} \rightarrow E_v$ and L2: $LUMO)_{GO_{epoxy}} \rightarrow E_v$, where LUMO-lowest unoccupied molecular orbital, GO_{epoxy}-epoxy groups of GO and E_v is the valance band of ZnO.[3] Besides, green emission is attributed to oxygen vacancies (V_Os) or zinc interstitials (Zn_is).[3]

In this report we highlight that the emission wavelengths of $Zn_i \rightarrow E_v$ and ex-$Zn_i \rightarrow E_v$ overlap with that of L1 and L2, respectively, where ex-Zn_i-extended Zn_is. Despite this, we do not rule out the earlier discussed transitions,[3] rather we report

[a]*UNAM-National Nanotechnology Research Centre, Bilkent University, Ankara, 06800, Turkey. E-mail: svempati01@qub.ac.uk*
[b]*Institute of Materials Science & Nanotechnology, Bilkent University, Ankara, 06800, Turkey*

on evidences of defect related and other emissions which have been largely ignored. Furthermore, the green emission in fact, is attributed to V_Os,[16–23] and consists of two components (bulk and depletion[16,17,19,23]), however, not to the presence of Zn_is. Since GO can be a p-type material (depending on the level of oxidation),[6,10,11] in the presence of ZnO it may form a depletion region and influence the emission characteristics as noted here. Furthermore, this report provides a general though vital mapping of crucial factors in analyzing the heterocombinations such as graphene (oxide) and inorganic semiconductors.

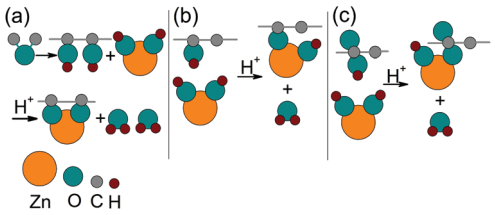

Fig. 1 Interaction between Zn^{2+} ion and (a) epoxy, (b) hydroxyl and (c) carboxyl groups of GO. Diagram not to scale.

Experimental

All the starting materials were received from Sigma and used as received. GO,[4,6,7] ZnO QDs,[3] and ZnO/GO QDs,[3] were synthesized as described in the given references. Additionally to reveal the influence of dimethyl formamide (DMF) we have treated GO with it (GO_{DMF}) at 95 °C for 5 h which matches the reaction conditions of ZnO/GO QDs without zinc acetate. These ZnO/GO QDs and GO_{DMF} were subjected to repeated washing with ethanol through centrifugation and finally with deionized water. All the samples were dried at 45 °C overnight under vacuum. Samples were subjected to transmission electron microscopy (TEM, FEI-Tecnai G2 F30) when dispersed in ethanol or deionized water and analyzed from a Cu-grid (without holey carbon coating). TEM images were processed with ImageJ (version 1.42q) software for their fast Fourier transform (FFT) counterparts. X-ray diffraction patterns (XRD) were obtained from a PANalytical X'pert Pro MPD ($\lambda_{Cu\text{-}K\alpha}$ = 1.5418 Å). The ionic state of elements at the surface of the samples was investigated by X-ray photoelectron spectroscopy (XPS, Thermoscientific K-alpha, $h\nu_{Al\text{-}K\alpha}$ = 1486.6 eV) with a flood-gun charge neutralizer. XPS peak deconvolution was performed with Avantage software. Raman spectroscopy was performed with WITec instruments (Alpha 300S, 532 nm laser). Emission responses were recorded from Horiba Scientific FL-1057 TCSPC at an excitation wavelength of ~350 nm. Optical emission (Gaussian, standard deviation (SD) ~2–3 nm), Raman spectra (Lorentzian, SD ~2 cm^{-1}) and XRD (Lorentzian, SD ~0.003°) were deconvoluted with OriginPro 8.5. Apart from the number of peaks, the other parameters were set as free until convergence except the center of two components of the green emission (fixed at 524 (C1) and 577 nm (C2)) based on knowledge from the literature.[16,17,19,23] The Raman peak in fluorescence spectra was fixed at ~378 nm for GO_{DMF}.

Results and discussion

The ionic interaction between Zn^{2+} ions and the oxygen-containing functional groups (–O–, –OH and –COOH) of GO is schematized in Fig. 1a–c, after Son *et al.*[3] The differences in the electronegativity/proton donating nature of these functional groups enable such an interaction with cations. Based on this interaction it can be suggested that ZnO QDs growth is initiated on GO where the oxygeneous functional groups are more dense. As a consequence it is expected that the ZnO QDs may not be entirely covered by GO. The effects of the uncovered ZnO are discussed in the emission properties. Contextually if the interaction between the adsorbate and substrate is much less than that of the adsorbed molecules themselves, then the influence of substrate on the superstructure can be ignored. In any case, the influence of the substrate on the superstructure will be evident in the structural investigation, *e.g.* XRD. Furthermore after the growth of the final structure ZnO QDs can host lattice defects, which if radiative, can be identified in photoluminescence (PL). Note that the site specific localized lattice defects will be spatially integrated over the probe beam area (XPS: ~400 μm^2, optical emission: ~8 mm^2, Raman: ~0.13 μm^2).

Representative TEM images of GO, ZnO QDs and ZnO/GO QDs are shown along with the FFT in Fig. 2. Probably a single layer of graphene suggests successful exfoliation of graphite while its wrinkles or folds are consistent with earlier reports.[4,6,7] The ZnO QD is shown as an inset of Fig. 2a. The lattice spacing is found to be ~2.25 Å, corresponding to the *c*-axis. A high resolution image from ZnO/GO QDs is shown in Fig. 2b. There are regions annotated with 1 and 2 which clearly show the honeycomb lattice of graphene. Earlier it was anticipated that ZnO QDs grow on graphene in which context we have selected two regions (3 & 4) for a closer inspection. At first glance, region 3 is darker than 4 presumably due to the differences in the electron transparency either because of the differences in the properties of the material and/or thickness. The FFT counterparts of regions 3 and 4 are shown on top of the selection on Fig. 2b. FFT of region 3 indicated two sets of intensities one of which corresponds to GO (hexagonal shaped, red dots) while the other to ZnO (blue dots). The FFT of region 4 depicted a pattern from the ZnO lattice while that of GO is not seen at an identifiable intensity level. Nevertheless, the presence of graphene is not denied in region 4, perhaps it may not be in focus due to possible wrinkles and/or folds. This analysis suggests that the ZnO QDs are in fact grown on GO sheets.

XRD-patterns from various samples are shown in Fig. 3 where the corresponding reflections are identified. GO has shown a single reflection depicting an interplanar spacing (d_{GO}) of ~8.379 Å which is consistent with the literature *vis-à-*

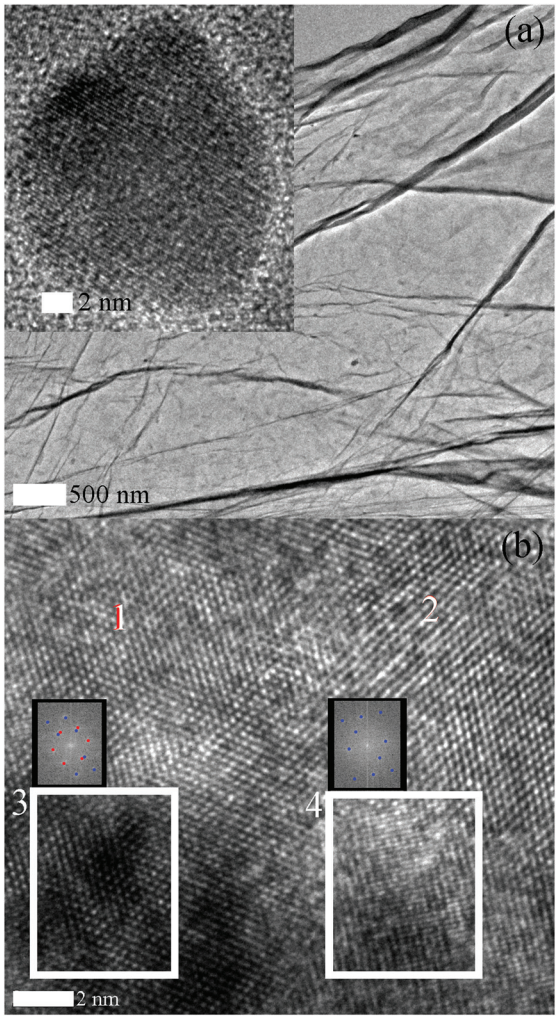

Fig. 2 TEM images of (a) GO, inset shows a ZnO QD (b) atomic resolved ZnO/GO QD, where FFT image of the boxed region (white) is shown. Red and blue spots correspond to graphene and ZnO lattices, respectively.

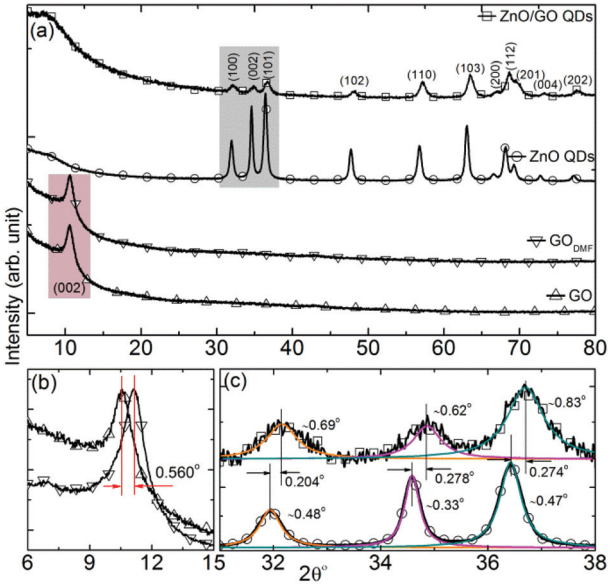

Fig. 3 XRD patterns from (a) GO, GO_{DMF}, ZnO QDs, ZnO/GO QDs (b) GO, GO_{DMF} (6–15°) and (c) ZnO QDs, ZnO/GO QDs (31–38°) with the fwhm values and angular shifts annotated.

vis $d_{graphite} \approx 3.368$ Å.[6,7] After oxidation the oxygeneous functional groups increase the distance between the graphene sheets which are otherwise stacked under the influence of van der Waal's force. The pattern from GO_{DMF} has sustained the (002) reflection, however, closer inspection of this peak (Fig. 3b) suggests a shift to a higher Bragg's angle than that of GO. It appears to be the case that the DMF treatment reduced some of the functional groups bringing the graphene sheets closer ($d_{GO_{DMF}} = \sim 7.968$ Å). The consequence of a lowered degree of oxidation may be reflected in fluorescence[2] and Raman spectroscopy. The pattern from ZnO QDs suggests a polycrystalline wurtzite structure and matches with the literature (Fig. 3a).[3,16,17,23] Furthermore (100), (002) and (101) reflections from ZnO containing samples are shown in Fig. 3c. A clear angular shift for ZnO/GO QDs to higher 2θ values results from the developed strain. A closer inspection of the full width at half maximum (fwhm) values of ZnO QDs and ZnO/GO QDs suggests sharper peaks for the former, in other words higher crystallite size. Furthermore, the peaks from ZnO/GO QDs did not appear to have shoulders at lower 2θ values which rules out the existence of uncovered ZnO QDs within the detection limits of XRD. This is convincing given the fact that Zn^{2+} ions are hoisted by the oxygeneous functional groups and the QD growth takes place on the surface of the GO sheets which is corroborated by TEM investigations. As speculated in the growth model, the 'substrate (GO) effect' is reflected in the angular shift of diffraction peaks. In the case of QDs there is not much of a 'bulk' formed due to their zero dimensions.[24] The absence of bulk material in fact results in a dramatic effect on its properties as the shift of 2θ corresponds to the whole material (high penetration depth of the probe X-rays[25]). In the case of the induced stress, additional effects can be expected on optoelectronic properties, in general.[26–28] Vacancies or other defects may be formed to relieve the interfacial strain.[29] Typically the surface stress (~1 N m^{-1}) is confined to a distance of 1 nm from the surface.[29] Nevertheless, in the course of ZnO/GO QDs synthesis, the possibility of formation of defects such as V_Os, Zn_is *etc.* are inevitable[3,30] which we will discuss in the context of PL. Furthermore, given the core (ZnO)–shell (GO) structure it is logical to expect an increase in the interplanar spacing of graphene or stress related effects on ZnO. However, no angular shifts for either (002) of GO or (100), (002) and (101) of ZnO were suggested in ref. 3. While, we have calculated lattice parameters (a and c) of zinc oxide from ZnO QDs and ZnO/GO QDs which are given in the following. $a_{ZnO\ QDs} = 3.235$, $c_{ZnO\ QDs} = 5.186$ Å and $a_{ZnO/GO\ QDs} = 3.215$, $c_{ZnO/GO\ QDs} = 5.147$ Å. It is apparent that the lattice parameters from ZnO/GO QDs are smaller than that of ZnO QDs. The quantitative changes (%) can be calculated by $[a(c)_{ZnO\ QDs} - a(c)_{ZnO/GO\ QDs}]/a(c)_{ZnO\ QDs}$ yielding ~0.62 and ~0.76% for a and c values, respectively.

The atomic percentages (at%) of the constituting elements from the each of the samples are tabulated in Fig. 4a. Core-level XP spectra of O 1s, C 1s and Zn 2p are shown in Fig. 4b–d, while the area ratios of O 1s and C 1s are annotated. We will discuss the C to O ratios later. From Fig. 4a ZnO QDs depict a slightly higher oxygen content than zinc which might be due to the chemisorbed oxygen (O_{Ch}) on the surface and V_Os.[31,32] In the case of ZnO/GO QDs the higher oxygen content can be from oxygeneous functional groups of GO. However, we expect some contribution from O_{Ch}. Carbon from ZnO QDs might have arose from atmospheric contamination, or glue from the copper tape that we used to load the samples into the analysis chamber, in addition to a fraction of residual starting materials. The same is true for ZnO/GO QDs, however additional contributions to the carbon comes from graphene. The energetic location of O 1s from ZnO (O_{ZnO}) is consistent with the literature (~530.4 eV, Fig. 4b).[17,31,33] O_{Ch} appeared at 532.2 eV indicating incorporation of –OH, –CO, adsorbed H_2O and/or O_2 or O^- and O^{-2} ions[17,33–35] essentially occupying the V_Os which play a critical role in the emission properties and related applications.[16,17,31,32]

C 1s spectra from GO, GO_{DMF}, ZnO/GO QDs suggested three oxygeneous functional groups (C–O, C=O and O–C=O) with varying fractions apart from C=C (Fig. 4c).[33] GO has depicted a ratio of C : O::0.82 : 1.44. During the oxidation process oxygeneous functional groups are implanted on the basal plane and edges of the graphene sheets.[7] This covalent functionalization increases the interplanar distance as evidenced in the XRD. Analysis on GO and GO_{DMF} suggest that total O at % decreased apart from some N incorporation presumably due to DMF treatment (GO_{DMF} C : O::1.38 : 1). It is also noted that a fraction of conversion of C=O to C–O may be originated from the protonation of carbonyls by $-CH_3$ groups of DMF. On the other hand, for the increase of O–C=O, the presence of –OH ions was attributed. It is convincing as we did not use anhydrous solvent in addition to the hydrophilic nature of GO. Further ZnO/GO QDs have shown C : O::1.93 : 1 which is higher than that of GO_{DMF}. In the former case, due to the presence of Zn^{2+} ions some of the functional groups are shielded in contrast to GO_{DMF}. This shielding hindered the access to DMF leaving the functional groups unreduced. We will see that in the context of Raman with a slightly increased interplanar spacing of GO due to the presence of ZnO QDs. The changes in the density of oxygeneous functional groups are consistent with the observation in XRD. In ref. 3 the analysis of O 1s core-level spectrum suggested fractional contributions are about 22% (C–O); 54% (O–C=O) and 22% (C=O) (Fig. S3–2, ESI of ref. 3). Due to the presence of DMF during the synthesis, C=O will be converted into C–O, apart from an increase in the O–C=O group. The presence of O–C=O groups in such high concentrations requires a full consideration in the context of opto-electronic properties which is not the case in ref. 3. On the other hand the presence of C=O functional groups (Fig. S3–2(b), ESI of ref. 3) is not discussed[3] in the context of interaction with Zn^{2+} in addition to its electron-trapping capability under an excited state.[4,36] These groups do interact with Zn^{2+} however, depending on the strength of the acidic nature.[6] The integral effect of all the existing oxygeneous functional groups form the QDs during the reaction.

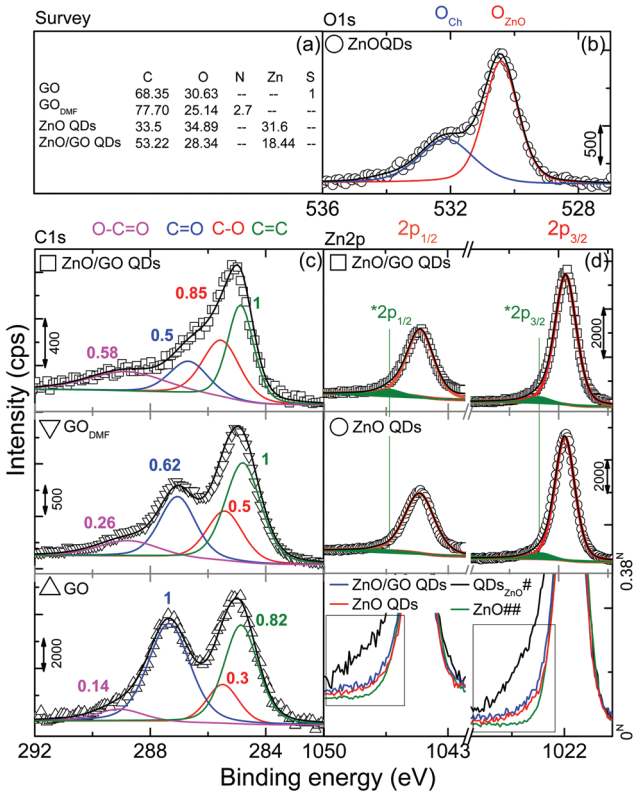

Fig. 4 (a) Atomic %, (b) O 1s from ZnO QDs, (c) C 1s from GO, GO_{DMF}, ZnO/GO QDs and (d) Zn2p from ZnO QDs, ZnO/GO QDs, normalized plot compares with ZnO. Data taken from the # ref. 17 and ## ref. 32. ^{N} normalized intensity scale.

Moving onto Fig. 4d, Zn 2p from ZnO QDs and ZnO/GO QDs were compared with literature.[17,32] For both the cases the doublet peak positions (Zn $2p_{3/2}$ and Zn $2p_{1/2}$ at ~1021.5 and ~1044.5 eV, respectively) and fwhm values match with the literature.[17,31–33] Apart from the Zn 2p doublet two additional peaks ($*2p_{3/2}$ and $*2p_{1/2}$ shaded in green) are observed at higher binding energies for both the samples. These peaks are attributed to the presence of Zn_is,[17,32,33] however, such a deconvolution of ionic state should be corroborated appropriately. In line with this we have co-plotted the normalized spectra from QDs_{ZnO}# and ZnO## where the former consists of significant density of Zn_is while the latter is a well developed grainy coating (data taken from the # ref. 17 and ## ref. 32). Zn_is are seen to occur in the presence of an inhomogeneous distribution of functional groups on the surface of the substrate[17] apart from Zn rich environments.[20] Interestingly, although at present the substrate is not the same as that of ref. 17 the interaction between the functional groups and Zn^{2+} appears to play a crucial role. Please consult ref. 17 for further details on synthesis and structure. The high energy tails of the Zn $2p_{3/2}$ and Zn $2p_{1/2}$ need to be inspected for

shoulder like structure (boxed region on Fig. 4d, bottom). In the case of QDs_{ZnO}# the shoulder at higher energy is quite clear. It is notable that the intensity of the shoulder decreases ZnO/GO QDs, ZnO QDs and ZnO## in that order. As we can see in the case of well developed and virtually defect free (Zn-related) surface there is no shoulder. This analysis essentially suggests the presence of Zn_is in ZnO/GO QDs and ZnO QDs of varying density which will be revealed through specific energy lines in the PL.

The Raman spectrum of GO is characterized by two main components, D and G bands. D-band: edges, defects or the breakdown of translational symmetry. G-band: first order scattering of E_{2g} phonon of sp^2 carbon atoms.[37] Raman response from GO, GO_{DMF} and ZnO/GO QDs are shown Fig. 5. Spectrum from GO has shown two signature peaks at ~1355 and ~1598 cm^{-1} corresponding to D and G bands, respectively. Interestingly the peak at ~1355 cm^{-1} did not show any significant spectral shift for the two modifications while the latter is shifted to ~1580 and ~1590 cm^{-1} upon DMF treatment and ZnO QDs growth process, respectively. It might be the case that the distance between the graphene sheets is decreased[37] (lowered density of oxygeneous functional groups) upon DMF treatment. However, due to the ZnO QDs and/or sustained degree of oxidation (interacting Zn^{2+}) the distance between the sheets is increased again and the G-band is recovered to an extent. However, this is not seen explicitly in the XRD due to relatively lower signal to noise ratio. It is not denied that the DMF treatment might increase the already established defects such as changing bond lengths, angle and disorder at the atomic scale which eventually softens the phonon modes.[37] If this is the case then the G-band may not recover to 1590 cm^{-1} for ZnO/GO QDs. Hence the softening of phonons is attributed to the decreased distance between the sheets rather than any other attribution. Note that the shift is not due to adsorbed DMF as no overlap of the peaks ('★' on Fig. 5) is seen within the detection limits. From Raman studies, it is also clear that the graphene in ZnO/GO QDs is not identical to that of GO_{DMF} in all aspects as expected due to the growth of ZnO QDs. Such changes in the degree of oxidation can be seen in the context of fluorescence properties.[2,5] Son *et al.*[3] noticed splitting of the G-band for ZnO/GO QDs (G^- and G^+ at 1566.6 and 1592.7 cm^{-1} respectively) and attributed it to uniaxial strain on graphene (monolayer) under a first order approximation.[38] In contrast to ref. 3 uniaxially bent graphene layer[38] has shown G^- and G^+ at ~1563 and ~1576 cm^{-1} (approximated from the plot), *i.e.* the G band splits and shifts to lower frequencies whereas G^+ has shown a significant blue shift of ~17 cm^{-1}. This shift cannot be attributed to the '*assumption*' of uniaxial strain[3] however biaxial strain is certainly closer to the ZnO/GO QDs case due to the spherical structure of QD. Nevertheless, in the case of biaxial strain no splitting is observed[39–41] apart from the red-shifted G-band.[39] Although biaxial strain better represents the core–shell configuration in ref. 3 the blue shift of G^+ might have arisen mainly due to ZnO. Notwithstanding, the presence of strain is not excluded in the current scenario. Contextually note that in the case of electron doping the G band blue shifts.[42] On the other hand, the presence of 3 at% of N might cause significant change in the electron density of GO thus the position of G band. Nevertheless, a deeper understanding of the influence of ZnO QDs under strain on the Raman modes of graphene is warranted.

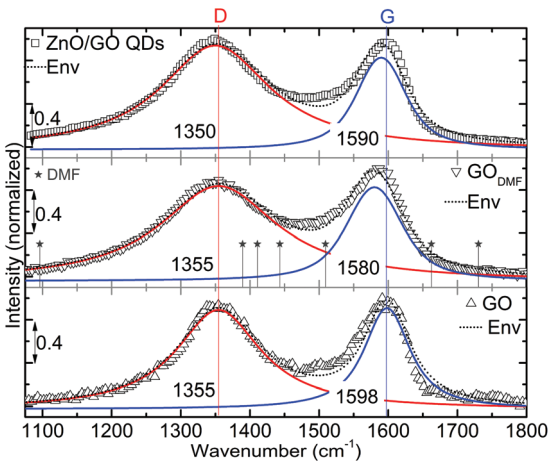

Fig. 5 Raman spectra from GO, GO_{DMF} and ZnO/GO QDs with peak deconvolution. Modes from pure DMF are denoted with ★. The spectral locations were annotated in cm^{-1}.

We have analyzed the emission properties of GO, GO_{DMF}, ZnO QDs and ZnO/GO QDs and plotted them in Fig. 6a–d respectively. L1 and L2 on part (b) indicate the spectral overlap of the emission peaks and hence are not to be attributed to Zn_is and ex-Zn_is. In ref. 3 the earlier mentioned lines, L1 and L2 are attributed to GO_{epoxy} and E_v transitions (intersystem crossings[3,15]), see Fig. 6e (E_c-conduction band and E_F-Fermi level). However, in XPS the presence of Zn_is and possible formation of ex-Zn_is is evidenced[3,30] while their emission is schematized in Fig. 6f. In what follows is a discussion of each of the samples in relation to the present attribution and the origin of the green emission. In general, the intrinsic lattice defects and surface states are predominant in QDs.[24] In the case of ZnO it is known that visible emission occurs from the surface[18,21,22] in which case, the extremely high surface area to volume ratio of QDs plays a critical role. To begin with, the fluorescence from GO is under intense discussion.[2,5] The peak annotated with R is due to Raman scattering which occurred at ~378 nm (~350 nm illumination) for both GO and GO_{DMF}. An overview of recent literature on the emission from GO and reduced-GO is given in ref. 2. Emission from GO is excitation dependent (see ref. 86–88 in ref. 2) and attributed to the various possible transitions from the minimum of the conduction band to localized states in the valance band. Basically the fluorescence from GO is explained based on two arguments. 1. The presence of oxygeneous functional groups on the basal plane. In this case the emission occurs from zigzag sites of GO where their ground state is in a triplet state similar to carbene, 2. quantum confinement of sp^2 domains (π-electrons) and e/h recombination therein. In this case, the local band gap depends on the size of the cluster. For GO_{DMF}

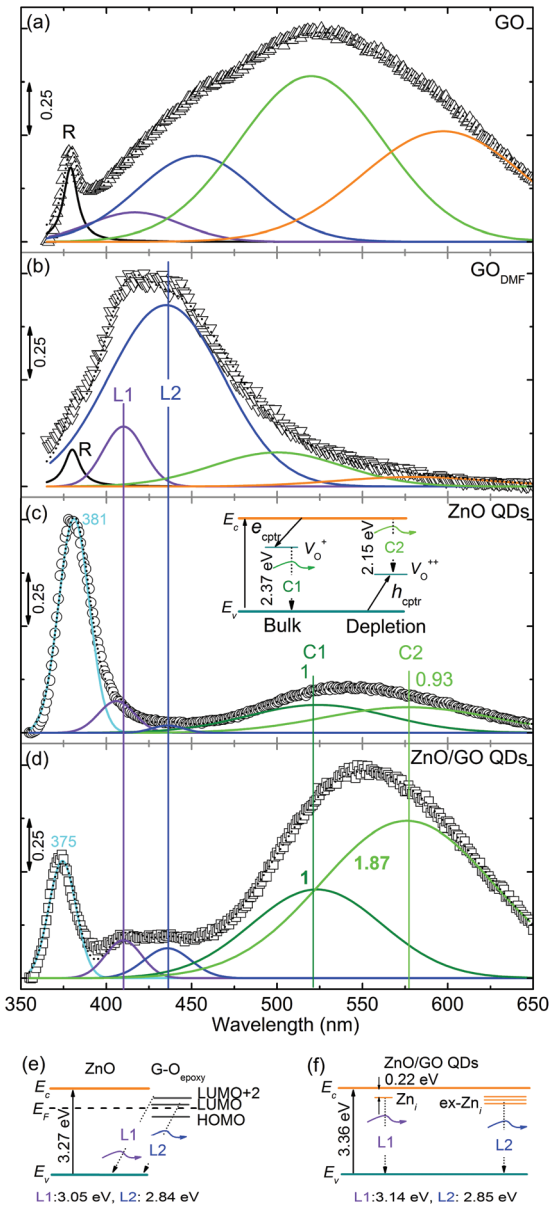

Fig. 6 Fluorescence from (a) GO, (b) GO_{DMF}, PL/optical emission from (c) ZnO QDs, (d) ZnO/GO QDs, (e) schematic of the two emission lines redrawn after Son *et al.*[3] and (f) ZnO/GO QDs with defect levels Zn_i and ex-Zn_i states, insert of (c) depicts the schematic of the green emission from ZnO. Area ratio is indicated with reference to that of 524 nm the (C1) peak in the respective sample. E_c, E_v are conduction and valance bands, respectively, while e_{cptr} and h_{cptr} are electron and hole capture processes, respectively, and E_F is the Fermi level. L1 and L2 on part (b) only indicate the spectral overlap of the emission peaks and hence should not be attributed to Zn_is and ex-Zn_is.

the reaction with DMF incorporated nitrogen (XPS and Raman) which can influence the emission characteristics *via* doping the GO. Going into specifics, for GO (Fig. 6a) two peaks are noted in the blue region at ~416 and ~452 nm (apart from two more components) which were slightly blue shifted to ~409 and ~434 nm respectively, for the GO_{DMF} case (Fig. 6b).[2] Based on the literature and the available explanation[2] we believe that these two blue emissions may be due to confinement of sp^2 domains. The blue shift of the blue emission may be due to increased confinement after DMF treatment. After DMF treatment the other two peaks at 520 and 597 nm have almost distinguished. This can be due to the overall decrease in the degree of oxidation, d value ($d_{GO} > d_{GO_{DMF}}$) and conversion of some functional groups.[2,5] Hence these higher wavelength peaks may be attributed to the oxygeneous functional groups. Interestingly the blue emission peaks from GO_{DMF} (~409 and ~434 nm) spectrally overlap with that of L1: $(LUMO+2)_{GO_{epoxy}} \rightarrow E_v$ at 406 nm and L2: $(LUMO)_{GO_{epoxy}} \rightarrow E_v$ at 436 nm from ref. 3. We wish to point out that the emission bands may be due to the GO_{DMF} juxtaposing with the proposed intersystem crossing. This spectral overlap is crucial to address and rule-out the possibility of emission from GO_{DMF}. The PL/optical emission spectra from ZnO QDs and ZnO/GO QDs are shown in Fig. 6c and d, respectively. The band gap of each sample is calculated as the sum of exciton emission and its binding energy (60 meV) yielding 3.31 eV and 3.36 eV for ZnO QDs and ZnO/GO QDs, respectively (Fig. 6f). The slight increase in the band gap can be attributed to the quantum confinement effect, in line with the earlier discussed growth mechanism. The 2D growth of ZnO on the surface of GO enhanced the confinement from pristine QDs. The green-emission from ZnO is attributed to V_Os consisting of two components. Specifically, C1: 524 nm (2.37 eV): $V_O^* \rightarrow E_v$, and C2: 577 nm (2.15 eV) $E_c \rightarrow V_O^{++}$, which take place in bulk and depletion regions, respectively (inset of Fig. 6c).[16,18,19,21–23,43] V_O^+ states either capture an electron (e) or hole (h) from E_c or E_v respectively, *i.e.* $V_O^+ + e \rightarrow V_O^*$ and $V_O^+ + h \rightarrow V_O^{++}$. Furthermore, the area ratios of C1 to C2 across the two ZnO containing samples are considered which reflect the emission from the corresponding regions. The ratios are $(C1 : C2)_{ZnO\ QDs}$::1 : 0.93; $(C1 : C2)_{ZnO/GO\ QDs}$::1 : 1.87. Explicitly in the ZnO/GO QDs sample there is almost a two-fold variation in the area of C2.[16,19] The enhanced C2 emission is convincing because of the fact that the GO[6,10,11] and ZnO[16,19] are p- (depending on the degree of oxidation) and intrinsic n-type materials, respectively. The volume of the depletion region is increased due to the presence of GO which enhances C2 as we observed here. Note that in the ZnO QDs case the occupancies of V_Os form the depletion region. To further comment on this, the observed changes in the relative emissions of C1 and C2 may not be an interfacial quenching, which requires a transfer of photoexcited electrons from E_c of ZnO to E_F of graphene.[44] In this case the whole emission is expected to decrease. However, we don't completely rule out such a possibility if the GO is sufficiently metallic within the interface.

In the blue region of ZnO QDs two peaks are seen, 405 nm (L1) and (435) L2 while the latter depicted relatively low intensity. Zn 2p core-level spectrum evidenced the presence of Zn_is in smaller density from ZnO QDs which is reflected in the PL. The above two lines are attributed to Zn_is and ex-Zn_is, respectively (L1: $Zn_i \rightarrow E_v$ and L2: ex-$Zn_i \rightarrow E_v$)[20] and consistent with the literature.[17,20,23] Zn_is are about 0.22 eV below the E_c,[45] while ex-Zn_is are ~0.5 eV below E_c.[20] Under suitable illu-

mination, electrons are excited to the E_c, which are then non-radiatively transitioned into Zn_is or ex-Zn_i. Also electron transfer can take place from Zn_is to ex-Zn_i and subsequently to E_v. These localized electrons recombine with free holes in the E_v leading to violet or blue emission.[20] The presence of GO prior to the formation of ZnO QDs has a significant influence on its growth, where the Zn^{2+} ions are anchored to the oxygeneous functional groups of GO. Also, during the growth GO-sheets enclose the QD either partially or completely (Fig. 2 and Fig. 2 of ref. 3). Although the GO sheets are flexible, XRD results suggest spatial or physical restriction that is imposed on interacting-Zn^{2+} ions which may cause lattice defects such as Zn_is on the surface.[17,20] Zn 2p core-level spectra suggest a slightly higher density of Zn_is in ZnO/GO QDs than that of ZnO QDs, which is clearly reflected in the emission. These Zn_is form ex-Zn_i states[20] as we can see the prominent difference in L2 across the two samples. For ZnO QDs, L1 due to Zn_is should occur at 3.09 eV which is at 3.05 eV with reference to the band gap (abbreviated as 'L1-ZnO QDs|Zn_is: 3.09/3.05 eV'). Similarly L2-ZnO QDs|ex-Zn_is: 2.8/2.86 eV, L1-ZnO/GO QDs|Zn_is: 3.14/3.03 eV and L2-ZnO QDs|ex-Zn_is: 2.85/2.85 eV. A small disagreement between the emitted and expected lines is due to the differences in the band gap, the error involved in the deconvolution procedure. Especially for ZnO/GO QDs it can be a combination with the fluorescence from GO. The presence of C=O functional groups may decrease the quantum efficiency of the ZnO/GO QDs by trapping the electrons under an excited state.[4,36] The consequences of trapping will be explicit in the context of optoelectronic properties as noted earlier.[4] However, the efficiency of trapping of photoexcited electrons is determined by its recombination dynamics and physical accessibility, *i.e.* the functional group must be fast enough to trap the electron before the recombination. It is also notable that the recombination dynamics are influenced by electron and hole mobilities against the intrinsic electric field due to the depletion layer. Given this the complete quenching of emission from ZnO due to C=O groups can be an ideal scenario. Furthermore, since emission is seen from ZnO/GO QDs, it is believed that the density of C=O was not high enough to quench the emission completely, where the DMF treatment has converted the C=O groups in to C–O groups. Earlier it was mentioned that the ZnO QDs are not fully covered by GO. However, the fraction of which can be very low and it would not undermine the discussion. The uncovered ZnO would not suppress the emission from ZnO/GO QDs rather we observe an integral effect from both uncovered ZnO and ZnO/GO QDs depending on their relative fractions. In the mixed case the peak area corresponding to the intrinsic defects cannot be simply attributed to individual constituents (when the exact fraction is unknown). Nevertheless, the defect emission wouldn't change its spectral position and should be evident in the PL. The existence of uncovered ZnO QDs in large fractions is unlikely, for instance the XRD of ZnO/GO QDs did not depict any peaks with shoulders, which shows the contribution from uncovered ZnO QDs. On the other hand, XRD evidenced significant stress on the ZnO lattice in ZnO/GO QDs, *viz.* the quantitative changes were ~0.62 and ~0.76% for *a* and *c* values, respectively. Xu *et al.*[26] suggested a piezotronic effect on the PL of ZnO nanowires (NWs) where excitonic emission red-shifts with increasing stress. Essentially the piezoelectric field ($\pm\varphi$) redistributes the photoexcited carriers along with a modified band structure of a bent ZnO NW causing a red-shift. The following parameters determine the presence of the piezotronic effect. (a) $|\varphi|$ critically depends on the doping density (N_D) while the latter can partially or totally screen the φ.[28] (b) For $W \ll d_{NW}$ the red-shift is independent of the d_{NW} where W – width of the depletion layer and d_{NW} – diameter of the nanowire. When $W \approx d_{NW}$ the red-shift is dependent on the d_{NW}, which decreases with decreasing d_{NW}[26] (c) single crystals depicted piezotronic[26] and piezoelectric response[27,28] (when bent along the *c*-axis) and highly *c*-axis oriented thin films[46] exhibited a piezoelectric response. In the present case we did not observe any piezotronic effect in the ZnO/GO QDs despite the strain due to the following reasons corresponding to the above factors. (a′) For ZnO, N_D is determined by point defects such as Zn_is and V_Os.[47] ZnO QDs consists of intrinsic defects (Zn_is and V_Os) as explicitly evidenced in the PL (Fig. 6c). The same is true for ZnO/GO QDs (Fig. 6d) where the defects are more pronounced and hence the relatively higher N_D screening the φ. (b′) For QDs, W is most probably as thick as the diameter. Moreover, W would be relatively higher for the ZnO/GO QDs case due to the p-natured GO (seen from the area ratios of green emission). Since $W \approx d_{NW}$ any shift is governed by the size of the QDs. From Fig. 5c of ref. 26, as the diameter of the NW decreases the red-shift of the free exciton emission decreases, essentially approaching $W \approx d_{NW}$. (c′) ZnO QDs and ZnO/GO QDs are polycrystalline without any preferential orientation. Piezotronic response is realized when a compressive strain is applied along the *c*-axis of NW[26,28] while *a* is allowed to modulate most probably increasing its value. Significantly, here *c* and *a* were subjected to compressive strain. It may be the case that the developed φ along one axis is compensated by the other axis. Furthermore, the φ may be compensated by GO, where there is a net supply of electrons from GO despite it being a p-type material.[6,10,11]

Conclusions

The ionic interaction between Zn^{2+} ions and the oxygeneous functional groups influence the growth of ZnO QDs, where the lattice of the latter is slightly compressed. Due to the previously mentioned interaction XPS evidenced Zn_is where their density in ZnO/GO QDs is higher than that of the pristine counterpart. Analyses of Raman spectra suggested a deeper investigation was needed to understand the influence of ZnO on GO. We do acknowledge the fact that the analysis of the optical emission from complex systems is not a simple arithmetic sum of two or more components, but involves various combinatory factors. Nevertheless, we provide direct conclusions with spectroscopic evidence on two vital issues regarding the mechanism of luminescence from the ZnO/GO composite. (i) L1 and

L2 have two alternative possibilities, *viz.* $Zn_i \rightarrow E_v$ and ex-$Zn_i \rightarrow E_v$ respectively and (ii) these two emissions might be from GO. The interaction between GO and Zn^{2+} is the basis for the existence of Zn_is as evidenced in the XPS and subsequently in PL. Also the presence of Zn_is can perhaps explain the emission from the light emitting diode structure in ref. 3. Under biased conditions the charge carriers may be injected from GO into the Zn_i or ex-Zn_i states which eventually recombine with free holes in the E_v emitting light of matching wavelength. Luminescence centered at 550 nm is attributed to V_Os with two components and a width of about 0.3 eV each in contrast to 0.8 eV shown in ref. 3. In the ZnO/GO QDs the emission from the depletion region is enhanced twice due to the presence of GO. The absence of the piezotronic effect in ZnO/GO QDs despite a significant strain is attributed to the increased N_D, $W \approx$ diameter of the QDs, compressive strain along *c* and *a* axes and to the presence of GO.

Acknowledgements

S. V. thanks The Scientific & Technological Research Council of Turkey (TUBITAK) (TUBITAK-BIDEB 2221-Fellowships for Visiting Scientists and Scientists on Sabbatical) for the postdoctoral fellowship. A. C. thanks to TUBITAK (Project no. 113Y348) for the postdoctoral fellowship. T. U. acknowledges The Turkish Academy of Sciences – Outstanding Young Scientists Award Program (TUBA-GEBIP).

Notes and references

1 A. M. Dimiev and J. M. Tour, *ACS Nano*, 2014, **8**, 3060–3068.
2 S. Vempati and T. Uyar, *Phys. Chem. Chem. Phys.*, 2014, **16**, 21183–21203.
3 D. I. Son, B. W. Kwon, D. H. Park, W. S. Seo, Y. Yi, B. Angadi, C. L. Lee and W. K. Choi, *Nat. Nanotechnol.*, 2012, **7**, 465–471.
4 S. Vempati, S. Ozcan and T. Uyar, *Appl. Phys. Lett.*, 2015, **106**, 051106.
5 K. P. Loh, Q. L. Bao, G. Eda and M. Chhowalla, *Nat. Chem.*, 2010, **2**, 1015–1024.
6 S. Vempati, A. Celebioglu and T. Uyar, *J. Mater. Chem. C*, 2014, **2**, 8585–8592.
7 D. C. Marcano, D. V. Kosynkin, J. M. Berlin, A. Sinitskii, Z. Sun, A. Slesarev, L. B. Alemany, W. Lu and J. M. Tour, *ACS Nano*, 2010, **4**, 4806–4814.
8 B. Yao, C. Li, J. Ma and G. Shi, *Phys. Chem. Chem. Phys.*, 2015, **17**, 19538.
9 P. Shao, J. Tian, B. Liu, W. Shi, S. Gao, Y. Song, M. Ling and F. Cui, *Nanoscale*, 2015, **7**, 14254.
10 R. J. W. E. Lahaye, H. K. Jeong, C. Y. Park and Y. H. Lee, *Phys. Rev. B: Condens. Matter Mater. Phys.*, 2009, **79**, 125435.
11 M. Jin, H.-K. Jeong, W. J. Yu, D. J. Bae, B. R. Kang and Y. H. Lee, *J. Phys. D: Appl. Phys.*, 2009, **42**, 135109.
12 S. Mondal, U. Rana and S. Malik, *Chem. Commun.*, 2015, **51**, 12365.
13 Q. Luo, Y. Zhang, C. Liu, J. Li, N. Wang and H. Lin, *J. Mater. Chem. A*, 2015, **3**, 15996.
14 Y. Wang, Y. Li, W. Qi and Y. Song, *Chem. Commun.*, 2015, **51**, 11022–11025.
15 S. S. Bao, Z. Hua, X. Y. Wang, Y. Zhou, C. F. Zhang, W. G. Tu, Z. G. Zou and M. Xiao, *Opt. Express*, 2012, **20**, 28801–28807.
16 S. Vempati, S. Chirakkara, J. Mitra, P. Dawson, K. K. Nanda and S. B. Krupanidhi, *Appl. Phys. Lett.*, 2012, **100**, 162104.
17 F. Kayaci, S. Vempati, I. Donmez, N. Biyikli and T. Uyar, *Nanoscale*, 2014, **6**, 10224–10234.
18 K. Vanheusden, C. H. Seager, W. L. Warren, D. R. Tallant and J. A. Voigt, *Appl. Phys. Lett.*, 1996, **68**, 403.
19 J. D. Ye, S. L. Gu, F. Qin, S. M. Zhu, S. M. Liu, X. Zhou, W. Liu, L. Q. Hu, R. Zhang, Y. Shi and Y. D. Zheng, *Appl. Phys. A: Mater. Sci. Process.*, 2005, **81**, 759.
20 H. Zeng, G. Duan, Y. Li, S. Yang, X. Xu and W. Cai, *Adv. Funct. Mater.*, 2010, **20**, 516–572.
21 A. v. Dijken, E. A. Meulenkamp, D. Vanmaekelbergh and A. Meijerink, *J. Phys. Chem. B*, 2000, **104**, 1715.
22 K. Vanheusden, W. L. Warren, C. H. Seager, D. R. Tallant, J. A. Voigt and B. E. Gnade, *J. Appl. Phys.*, 1996, **79**, 7983.
23 S. Vempati, J. Mitra and P. Dawson, *Nanoscale Res. Lett.*, 2012, **7**, 470.
24 S. Vempati, Y. Ertas and T. Uyar, *J. Phys. Chem. C*, 2013, **117**, 21609–21618.
25 X-ray penetration depth ($1/e$ of intensity, δ) = $1/(\xi\rho)$, where ρ-density (g cm^{-3}) and ξ-mass attenuation coefficient (cm^2 g^{-1}). ξ was taken from [http://physics.nist.gov/PhysRefData/XrayMassCoef/tab3.html]. ξ_{Zn} = 58.75, ξ_O = 11.63, $\xi_{ZnO} = \xi_{Zn} + \xi_O$, ρ_{ZnO} = 5.61; $\xi_{graphite}$ = 4.57, $\rho_{graphite}$ = 2.27; yielding δ_{ZnO} = ~25 μm and $\delta_{graphite}$ = ~960 μm.
26 S. Xu, W. Guo, S. Du, M. M. T. Loy and N. Wang, *Nano Lett.*, 2012, **12**, 5802–5807.
27 B. Wei, K. Zheng, Y. Ji, Y. Zhang, Z. Zhang and X. Han, *Nano Lett.*, 2012, **12**, 4595–4599.
28 Z. L. Wang, *J. Phys. Chem. Lett.*, 2010, **1**, 1388–1393.
29 H. Luth, *Solid Surfaces, Interfaces and Thin Films*, Springer, 5th edn, 2010, ISBN 978-3-642-13591-0, e-ISBN 978-3-642-13592-7, DOI: 10.1007/978-3-642-13592-7.
30 S. Niyogi, E. Bekyarova, M. E. Itkis, J. L. McWilliams, M. A. Hamon and R. C. Haddon, *J. Am. Chem. Soc.*, 2006, **128**, 7720–7721.
31 F. Kayaci, S. Vempati, C. O. Akgun, I. Donmez, N. Biyikli and T. Uyar, *Appl. Catal., B*, 2015, **176–177**, 646–653.
32 F. Kayaci, S. Vempati, C. O. Akgun, I. Donmez, N. Biyikli and T. Uyar, *Nanoscale*, 2014, **6**, 5735–5745.
33 A. V. Naumkin, A. K. Vass, S. W. Gaarenstroom and C. J. Powell, 2012, NIST Standard Reference Database 20, Version 4.1.
34 M. Chen, X. Wang, Y. Yu, Z. Pei, X. Bai, C. Sun, R. Huang and L. Wen, *Appl. Surf. Sci.*, 2000, **158**, 134–140.

35 A. Stănoiu, C. E. Simion and S. Somăcescu, *Sens. Actuators, B*, 2013, **186**, 687–694.
36 H. Chang, Z. Sun, Q. Yuan, F. Ding, X. Tao, F. Yan and Z. Zheng, *Adv. Mater.*, 2010, **22**, 4872.
37 A. C. Ferrari, *Solid State Commun.*, 2007, **143**, 47–57.
38 T. M. G. Mohiuddin, A. Lombardo, R. R. Nair, A. Bonetti, G. Savini, R. Jalil, N. Bonini, D. M. Basko, C. Galiotis, N. Marzari, K. S. Novoselov, A. K. Geim and A. C. Ferrari, *Phys. Rev. B: Condens. Matter Mater. Phys.*, 2009, **79**, 205433.
39 J. Zabel, R. R. Nair, A. Ott, T. Georgiou, A. K. Geim, K. S. Novoselov and C. Casiraghi, *Nano Lett.*, 2012, **12**, 617–621.
40 F. Ding, H. Ji, Y. Chen, A. Herklotz, K. Dorr, Y. Mei, A. Rastelli and O. G. Schmidt, *Nano Lett.*, 2010, **10**, 3453.
41 C. Metzger, S. Remi, M. Liu, S. V. Kusminskiy, A. H. N. Castro, A. K. Swan and B. B. Goldberg, *Nano Lett.*, 2010, **10**, 6.
42 S. Pisana, M. Lazzeri, C. Casiraghi, K. S. Novoselov, A. K. Geim, A. C. Ferrari and F. Mauri, *Nat. Mater.*, 2007, **6**, 198.
43 M. Ghosh and A. K. Raychaudhuri, *Nanotechnology*, 2008, **19**, 445704.
44 E_F equilibration takes place when the materials are brought into contact.
45 C. H. Ahn, Y. Y. Kim, D. C. Kim, S. K. Mohanta and H. K. Cho, *J. Appl. Phys.*, 2009, **105**, 013502.
46 I. K. Bdikin, J. Gracio, R. Ayouchi, R. Schwarz and A. L. Kholkin, *Nanotechnology*, 2010, **21**, 235703.
47 Y. Gao and Z. L. Wang, *Nano Lett.*, 2009, **9**, 1103–1110.